Monolithically integrated refractive microlens standing perpendicular to the substrate

C. R. King, L. Y. Lin, and M. C. Wu

UCLA, Electrical Engineering Department
405 Hilgard Avenue, Los Angeles, CA 90095-1594

ABSTRACT

We report the first fabrication of a spherical microlens monolithically integrated on a surface-micromachined supporting plate standing perpendicular to the substrate. The focusing and collimating abilities of the lens are successfully demonstrated.

Keywords: microlens, photoresist reflow, free-space micro-optical bench, integrated micro-optics, surface micromachining

1. INTRODUCTION

The integration of refractive lenses into free-space micro-optical systems is an important step towards applying the micro-optic bench approach to systems in optical data storage, sensing, communications networks, display, and packaging of optoelectronic devices. To interface with a variety of monolithically-integrated surface-micromachined components in an optical signal routing system (such as lenses, beam splitters, mirrors, gratings, and so on), the beam must travel parallel to the substrate, with each component necessarily mounted perpendicular so as to intercept the beam. Refractive microlenses have been in use for some time in various forms, but until now have always been either mounted directly onto, or else etched into, the surface of a substrate. Our design implements the refractive microlens on a supporting plate, allowing for rotation of the lens up from the substrate surface, and allowing for precise positioning of the lens perpendicular to the substrate.

Our previous work with surface-micromachined micro-optics has employed out-of-plane micro-Fresnel lenses[1,2]. These diffractive lenses are fabricated directly on the micromachined polysilicon plates. The design of the Fresnel lens is wavelength-specific. Despite their excellent optical performance, the lenses impose a low diffraction efficiency, 10% for binary-amplitude Fresnel lenses and 40% for binary-phase lenses. Therefore, easily manufacturable, out-of-plane refractive microlenses are highly desirable for high-performance free-space integrated micro-optical systems.

2. FABRICATION

The design consists of a reflowed-photoresist microlens mounted on a supporting plate. The support plate is held perpendicular to the substrate by integrated micro-spring latches and separate side-latches. The entire assembly is fabricated in a two-step process: surface-micromachining of the support-plate structure, which was carried out at the Microelectronic Center in North Carolina (MCNC) for this device, and subsequent deposition of the microlens onto the plate. The supporting structure is implemented using the standard surface micromachining steps of depositing alternate layers of polysilicon and phospho-silicate glass (PSG), with patterned etches of the PSG layers defining contacts

between the polysilicon layers and between the polysilicon and the substrate, which is covered with a layer of silicon nitride. The PSG acts as a sacrificial mold for proper placement of the polysilicon contacts, and is ultimately removed by soaking the chip in HF, which frees the structures defined on the polysilicon layers (a process known as *releasing*). This design uses the second overlapping polysilicon layer to implement hinges[3], which restrain the support plate and side latches to the substrate, and to provide a catch mechanism for the spring-latches on the body of the plate. The side-latches are separate plates with thin V-shaped wedges which allow them to slide down the edge of the support-plate. They are included to provide better mechanical strength for the device and to precisely define the 90° angle with the substrate. The plate's location is specified in the layout of the chip, which allows positioning of components with 1 μm accuracy. The lens is positioned on the plate so as to provide the desired orientation in free-space after the plate is rotated up from the surface.

The microlens is deposited on the support plate prior to the releasing step, when the plate and side-latches are still confined by the PSG on the chip. Two successive layers of AZ 4620 Photoresist are spun onto the chip, resulting in a thickness of up to 20 μm. Photolithography is used to define a circle of 300 μm diameter, properly positioned over the support plate. Exposure and development steps result in the removal of all the remaining photoresist. At this point there is a cylinder of photoresist on the plate. The chip is then placed in a convection oven at 200 °F for 20 minutes, causing reflow of the photoresist, which takes on a spherical surface shape due to surface tension forces. An advantage of AZ 4620 over some other resists used for microlens manufacture[4,5,6] is its resistance to spreading during reflow—the lens maintains a constant diameter.

After cooling down, the structure is released in HF and then assembled manually at a probe station. A SEM micrograph of the final structure is shown in Fig. 1. Also see Fig. 5 .

Figure 1 SEM micrograph of the fully assembled refractive microlens. The device has been coated with a layer of gold to produce an image free from the distortion resulting from charge collection on the lens. The lens is 300 μm in diameter.

Note the holes visible in the support plate shown in Fig. 1—these are included to improve the etch rate during the release step. For this device, the holes are present over the entire surface of the support plate, even under the lens surface. At the time of manufacture of the initial device, the support plate structure was available on a chip from previous work. The presence of the etch holes under the surface of the lens is not desired, however, as they constitute aberrations in the bottom lens surface, and result in a slight degradation of lens performance.

3. CHARACTERIZATION

The material used to fabricate the lens must have the ability to reflow to a closely spherical surface as well as the property of low absorption for the desired wavelength. The results of a Tencor Alpha-Step 200 Profilometer scan of the plate-mounted lens are shown in Fig. 2. The profilometer results are consistent with a spherical surface with a radius of curvature of 432 μm, referenced to the center height (sag height). The departure from a perfectly spherical surface is plotted in Fig. 3. The data show that the lens has a surface which is spherical to within less than 0.5 μm over a central radius of 110 μm. This tendency for the surface to be a better approximation to a sphere over its central area is typical for microlenses. For this reason, many microlenses are designed with integrated apertures to restrict the beam to the central portions of the lens[4,5].
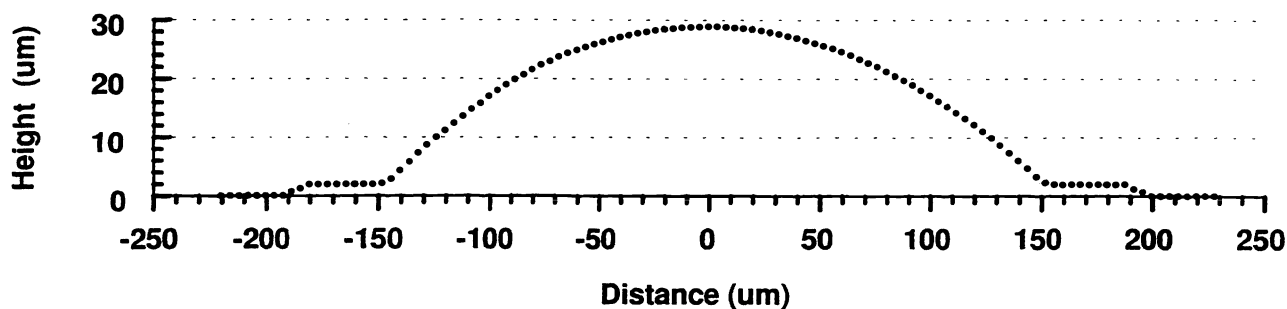
Figure 2 Surface profile of the plate-mounted lens. Note the inequality of vertical and horizontal scales. The profile of the support-plate is present adjacent to the sides of the lens.
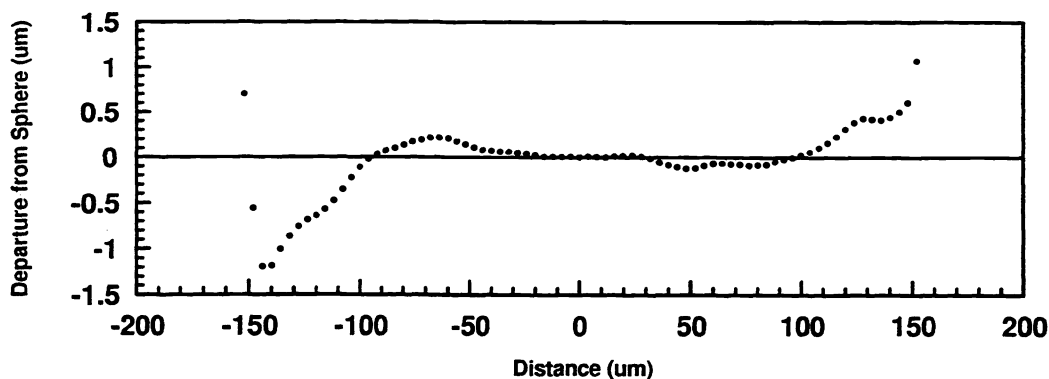
Figure 3 Departure from a spherical surface profile for the lens surface.

To determine the absorption coefficient of the AZ 4620 photoresist, several glass slides with different thicknesses of the resist were prepared, and subjected to the same reflow process as the lens. The intensity of a red HeNe laser beam (λ = 633 nm) was measured after passing through different thicknesses of resist.

The beam intensity after passing through the resist (I_f) is determined by the intensity incident on the glass slide (I_0), the transmission coefficient of the glass slide (T), the absorption coefficient of the resist (α), and the thickness of the resist (t), according to the formula:

$$I_f = I_0 T exp(-\alpha t) ,$$

which yields the linear relation:

$$Ln(I_0/I_f) = \alpha t - Ln(T) .$$

Data is plotted in this manner in Fig. 4. The value of the absorption coefficient, as determined from the slope of the line, is $\alpha = 0.0122 \ \mu m^{-1}$, or $\alpha = 0.0532 \ dB/\mu m$.
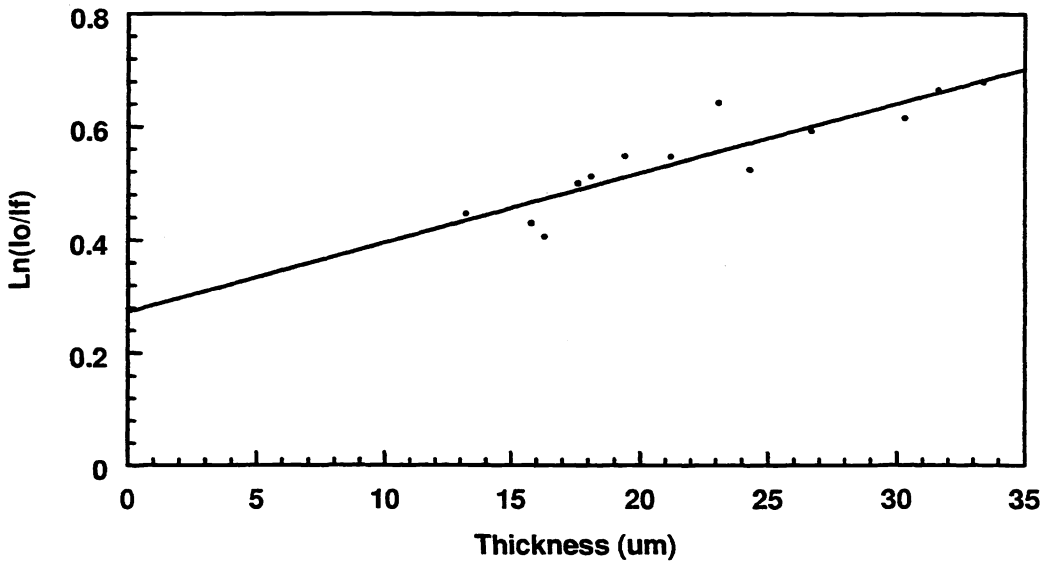
Figure 4 Absorption vs. thickness of AZ 4620 photoresist.

The optical loss through the lens, using this value of absorption coefficient, is estimated to be 0.72 dB, or a loss of intensity of approximately 15%. This value was obtained by taking the thickness of a cylinder of equal volume to the lens as a path length for propagation.

Applying the calculated radius of curvature (R_c) of 432 μm and the reference value for the index of refraction for AZ 4620 of n = 1.6176 to the equation for focal length $f = R_c/(n - 1)$ yields an expected focal length for the lens of f = 699 μm.

4. TESTING

Testing of the performance of the lens was conducted to determine the collimating ability, focal length, and minimum focal spot size. A red HeNe laser was coupled to a single-mode fiber and used to illuminate the plate supporting the lens. The fiber was positioned so as to provide a collimated output, as shown in the schematic in Fig. 5. An intensity profile of the collimated beam is shown in Fig. 6.
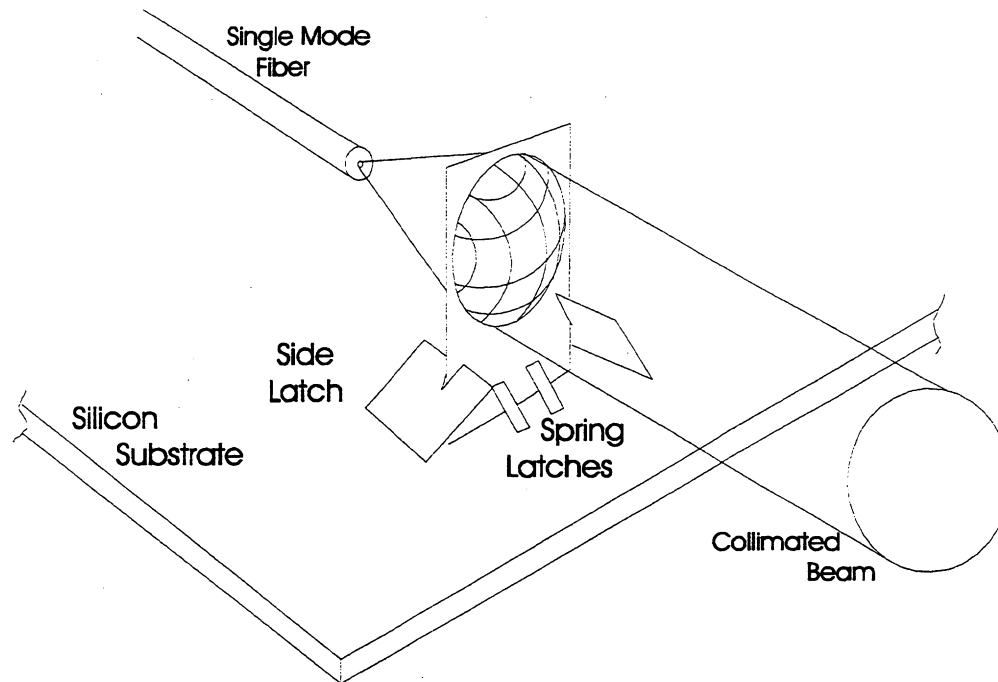
Figure 5 Schematic of the experimental setup for the measurement of deviation angle.
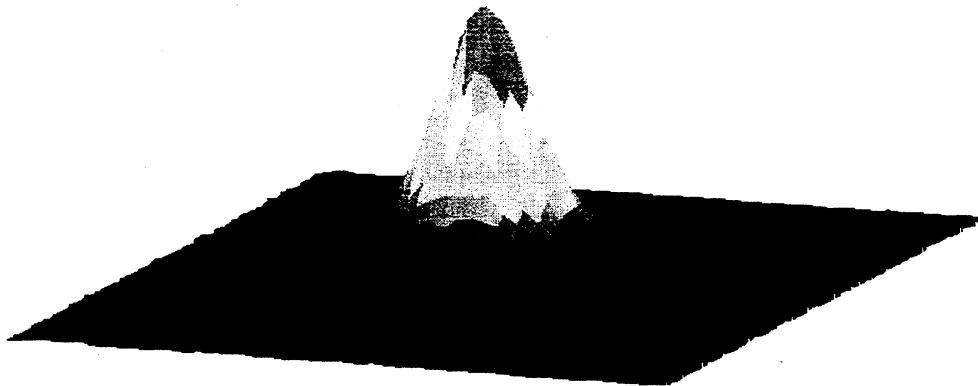
Figure 6 Three-dimensional profile of the collimated beam intensity.

The collimated beam width (FWHM) was measured over a range of distance from the lens using a CCD camera, and the data is plotted in Fig. 7. Data was taken for the fiber without the lens in the beam, and for the beam collimated by the lens. The plot yields a divergence angle for the collimated beam of 0.18°, compared to an angle of 3.3° for the fiber alone.
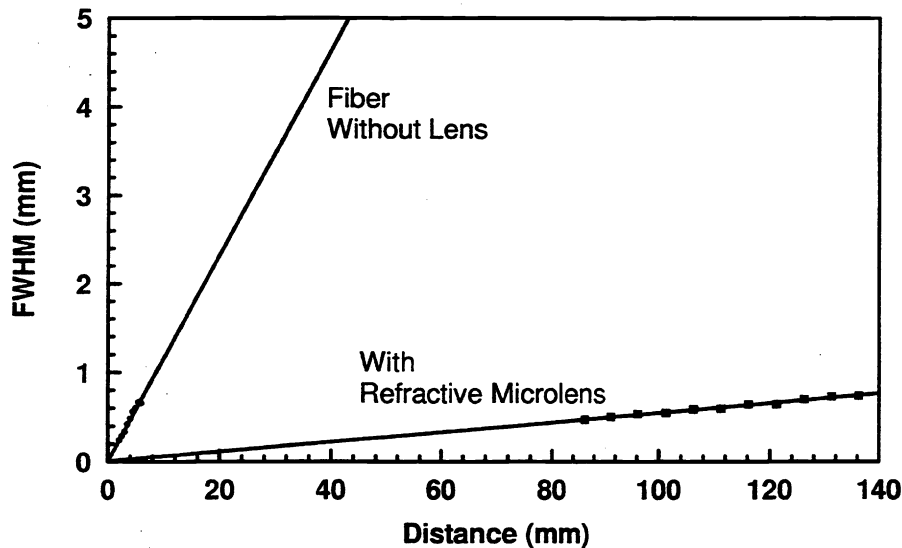
Figure 7 Beam width (Full Width at Half Maximum) vs. Distance, using a single-mode optical fiber both with and without the microlens.

The experiment also yields a value for the focal length of the lens, based on the distance between the fiber tip and the lens plate. This was measured as 637 μm.

To measure the focal spot size for the beam focused by the plate-mounted lens, the red HeNe laser output was coupled to the single mode fiber. To provide a collimated input to the plate-mounted lens, separate lenses of equal design parameters were fabricated, but were mounted on a glass slide. The optical fiber was positioned to provide a collimated beam from the output of the lens mounted on the glass slide. This beam was incident upon the plate-mounted lens, and the focal spot size was measured with a CCD camera. The measured FWHM spot size of 2.2 μm compares to a theoretical diffraction-limited spot size of 1.3 μm. This theoretical limit was arrived at by calculating the FWHM of the Airy disk produced by diffraction from a circular aperture of equal diameter to the lens, given by the equation $d = 2.44 \lambda \ f/\#$.

5. APPLICATIONS AND DESIGN PARAMETER CONSIDERATIONS

The focal length of the lens in this design process is determined by the initial thickness of the photoresist layer and the diameter of the lens, which is defined by the mask used to expose the resist. The resist thickness required for a given radius of curvature (R_c) for the lens (which defines the focal length), may in principle be calculated by equating the volume of the spherical portion representing the final lens shape to the volume of a cylinder representing the photoresist column before reflow[7]. For the lens represented as a section of a perfect sphere, the volume is given by $(\pi/3)H^2(3R_c - H)$, where H

represents the lens sag, and R_c is the radius of curvature of the lens. The relation between R_c and H, as provided in ref. [7], is $R_c = H/2 + D^2/8H$, where D is the diameter of the lens. A constant term (β) must be included to account for the loss of volume due to the evaporation of solvents during reflow. Equating volumes, then, we have $(\pi/3)H^2(3R_c - H) = \beta\pi t(D^2/4)$, where t is the thickness of the photoresist layer before reflow. This expression allows us to solve for t in terms of R_c, which is in turn specified by the desired focal length and lens diameter.

Determination of the value of the constant β is thus critical for design purposes; if its value is known, then the proper thickness of the photoresist layer to produce a lens with a given focal length can be determined precisely. In practice, however, measurement and use of the constant is problematic, particularly if more than one layer of photoresist is required to achieve the desired thickness. The nature of the problem is that of partial evaporation of the solvents before measurement of the thickness of the photoresist layer.

The effect of working with only an approximate value of β may impose restrictions on some applications. On-chip collimation of the beam from a fiber-optic cable is readily accomplished, since the end of the cable may be freely moved to the proper focal length from the lens. Focusing of a light beam for coupling into a cable may be similarly accomplished. The lens may not be so easily extended into applications involving the collimation of light from a laser diode, which requires the diode to be properly positioned at a focal length's distance from the lens. If the laser diode is pre-positioned on the chip in the design layout, proper coupling to the refractive lens may require that the lens be mounted on a moveable plate.

Apart from the determination of a practical value for β, it is of course necessary to have precise control over the thickness of the applied photoresist layers, as both of these parameters influence the resulting focal length of the lens after reflow.

6. CONCLUSION

In summary, the inclusion of refractive lenses constitutes an important advancement for the micro-optic bench approach to optical systems. The novel mounting system allows for monolithic integration of the refractive lens onto silicon chips, and can be used in the implementation of free-space optical interconnects, optical switches, and optical storage systems.

The refractive micro-lens offers a great improvement in efficiency over diffractive Fresnel-plate lenses, and has the additional attraction of not being wavelength-restricted in design. The Fresnel-plate lens does retain significant advantages, however. It requires no post-processing work, which is necessary for the lens deposition and reflow of the plate-mounted refractive lens. Another advantage of the Fresnel-plate lens is greater control of the focal length of the lens during the design process.

7. ACKNOWLEDGMENT

8. REFERENCES

1. L. Y. Lin, S. S. Lee, K. S. J. Pister, and M. C. Wu, "Micro-machined three-dimensional micro-optics for integrated free-space optical system," IEEE Photonics Tech. Lett., Vol. 6, No. 12, pp. 1445-47, 1994.
2. L. Y. Lin, S. S. Lee, K. S. J. Pister, and M. C. Wu, "Three-dimensional micro-Fresnel optical elements fabricated by micromachining technique," Electron. Lett., Vol. 30, No. 5, pp. 448-49, 1994.
3. K. S. J. Pister, M. W. Judy, S. R. Burgett, and R. S. Fearing, "Microfabricated hinges," Sensors and Actuators A, Vol. 33, pp. 249-256, 1992.
4. Z. D. Popovic, R. A. Sprague, and G. A. Neville Connell, "Technique for monolithic fabrication of microlens arrays," Applied Optics, Vol. 27, No. 7, pp. 1281-84.
5. N. J. Phillips, C. A. Barnett, "Micro-optic studies using photopolymers," *Proceedings of SPIE*, Vol. 1544, Miniature and Micro-Optics, pp. 10-21.
6. E. M. Strzelecka, G. D. Robinson, M. G. Peters, F. H. Peters and L. A. Coldren, "Monolithic integration of vertical-cavity laser diodes with refractive GaAs microlenses," Electron. Lett., Vol. 31, No. 9, pp. 724-25.
7. T. R. Jay, M. B. Stern, R. E. Knowlden, "Effect of refractive microlens array fabrication parameters on optical quality," *Proceedings of SPIE*, Vol. 1751, Miniature and Micro-Optics, pp. 236-45.